Michigan State University

National Superconducting Cyclotron Laboratory

COLLECTIVITY IN ^{44}S

T. GLASMACHER, B.A. BROWN, M.J. CHROMIK, P.D. COTTLE, M. FAUERBACH, R.W. IBBOTSON, K.W. KEMPER, D.J. MORRISSEY, H. SCHEIT, D.W. SKLENICKA, and M. STEINER

MSUCL-1048 **January 1997**

MSUCL 1048, submitted to Phys. Lett. B

Collectivity in ^{44}S

T. Glasmacher[1,2], B.A. Brown[1,2], M.J. Chromik[1,2], P.D. Cottle[3], M. Fauerbach[1,2], R.W. Ibbotson[1], K.W. Kemper[3], D.J. Morrissey[1,4], H. Scheit[1,2], D.W. Sklenicka[1*], and M. Steiner[1]

[1] *National Supercond. Cyclotron Laboratory, Michigan State University, East Lansing, MI 48824*

[2] *Department of Physics and Astronomy, Michigan State University, East Lansing, MI 48824*

[3] *Department of Physics, Florida State University, Tallahassee, Florida 32306*

[4] *Department of Chemistry, Michigan State University, East Lansing, MI 48824*

(January 14, 1997)

Abstract

The energy and reduced transition probability $B(E2; 0^+_{g.s.} \rightarrow 2^+)$ for the lowest excited state in the neutron-rich isotope $^{44}_{16}S_{28}$ were measured by intermediate-energy Coulomb excitation. The excitation energy is $E(2^+) =$ 1297(18) keV and the reduced transition probability is $B(E2; 0^+_{g.s.} \rightarrow 2^+_1) =$ 314(88) e^{2}fm^4. The experimental results are compared with self-consistent mean field calculations and shell model calculations with empirical interactions. The shell model calculations indicate that the large $B(E2)$ value in ^{44}S is vibrational in origin, while the neighboring isotopes ^{40,42}S are statically deformed.

27.40.+z,21.60.Cs,25.70.De,27.30.+t

Typeset using REVTEX

*Permanent address: Drake University, Physics and Astronomy Dept., Des Moines, IA 50311

In this letter, we report the first measurement of the energy and reduced transition probability $B(E2; 0^+_{g.s.} \rightarrow 2^+)$ of the lowest 2^+ state in the neutron-rich radioactive $N = 28$ isotope ^{44}S. This state was excited with the technique of intermediate-energy Coulomb excitation of a radioactive ^{44}S beam having an intensity of only approximately 15 particles/s. The results indicate that the 2^+_1 state in ^{44}S has a collective nature. With the present measurement, the chain of even-Z $N = 28$ isotones with measured electromagnetic matrix elements $B(E2; 0^+_{g.s.} \rightarrow 2^+)$ has been extended from iron ($Z = 26$) to sulfur ($Z = 16$), allowing a systematic understanding of the effects of the $N = 28$ major shell closure on the structure of these nuclei. With the sole exception of ^{48}Ca, the $N = 28$ isotones are collective, though generally not as much as ^{44}S. We compare the present data on ^{44}S and previously reported data on neighboring nuclei to self-consistent mean field calculations by Werner *et al.* [1] and to our own shell model calculations using empirical interactions obtained from nuclei close to the beta-stability line.

Intermediate-energy Coulomb excitation [2] of radioactive beams has been used recently to populate low-lying states of ^{38,40,42}S and ^{44,46}Ar [3], as well as states in several $A \leq 14$ nuclei [4] and ^{32}Mg [5]. The work reported here was performed at the National Superconducting Cyclotron Laboratory at Michigan State University. A primary beam of $^{48}Ca^{12+}$ at an energy of 70 MeV/nucleon and an intensity of 25 *particle*-nA was produced with the NSCL room temperature electron cyclotron resonance ion source and the K1200 cyclotron. The high intensity ^{48}Ca beam was produced by online reduction from CaO (enriched to about 70% in ^{48}Ca) with the technique described in [6]. The secondary ^{44}S beam was obtained via projectile fragmentation in a 379 mg/cm^2 ^{9}Be primary target located at the mid-acceptance target position of the A1200 fragment separator [7]. A thin degrader (10 mg/cm^2 carbon) was placed at the second intermediate dispersive image of the A1200 to reduce the number of light fragments that reach the A1200 focal plane and subsequently the experimental setup. The magnetic field settings of the A1200 fragment separator were optimized for the transmission of ^{44}S. Since the production cross section (four proton stripping) for ^{44}S is very small, its yield at the experimental station was approximately 15 particles/s and accounted for only about 0.4% of the secondary beam fragments which reached the Coulomb excitation target. The mixed beam allowed the simultaneous measurement of Coulomb excitation of many different fragments, as the isotopes were identified event-by-event during the off-line analysis. Positive mass and element identification of each fragment came from the measurement of the time of flight between a thin plastic scintillator located after the A1200 focal plane and a parallel plate avalanche counter (PPAC) located in front of the secondary target in addition to a measurement of the fragment's energy loss/total energy in a cylindrical fast/slow plastic phoswich detector located after the secondary target. This 0°-detector restricted the observed range of beam particles scattered from the 533 mg/cm^2 secondary ^{197}Au target to have laboratory scattering angles of less than θ_{lab}=4.05° and thus provided an almost exclusive selection of Coulomb excited nuclei (due to the small cross section for nuclear excitation at such forward angles [3]). A schematic view of the detector arrangement in the secondary target area is shown in fig. 1.

Photons were measured in coincidence with the scattered secondary beam particles in an array of 38 position sensitive NaI(Tl) detectors [8]. The NaI(Tl) crystals were cylindrical, 18 cm long, 5.75 cm in diameter, enclosed in 0.45 mm thick aluminum shields. The detectors were oriented parallel to the beam direction around a 10.2 cm diameter beam pipe in three concentric rings, and the target was located at the midpoint of the detectors. Photomultiplier tubes were located at both ends of each detector, and the coincident signals from the two photomultiplier tubes were used to determine both the energy of the detected photon and the location of the photon interaction in the detector. Several γ-ray sources (^{22}Na, ^{88}Y, ^{152}Eu and ^{228}Th) were used to establish position-dependent energy calibrations and efficiencies of each detector. The energy resolution of the detectors was typically 8% at 662 keV, and the position resolution was approximately 2 cm, providing an angular resolution of better than 10° for each detected photon. The angular information was used to correct for the large Doppler shifts of the photons emitted from the secondary beam. The entire NaI(Tl) array was shielded from photons produced in the phoswich detector and PPACs, and from room background by a 16.6 cm layer of low-background lead bricks. The time difference between the detection of a photon in the NaI(Tl) detectors and the detection of the secondary beam particle in the phoswich detector was recorded for each event to reduce accidental coincidences.

The photons emitted from secondary beam particles, which had velocities of approximately $v = 0.276c$ (corresponding to a secondary beam energy of 35 MeV/nucleon in the middle of the gold target), could be distinguished from those from the ^{197}Au target by their Doppler shifts. Figure 2 shows the γ-ray spectrum in coincidence with ^{44}S in the laboratory-frame (no Doppler correction) and in the Doppler-shifted frame of the projectile. The laboratory-frame spectrum clearly shows a peak from the 547 keV γ-ray corresponding to the $7/2^+ \rightarrow g.s.$ transition in the ^{197}Au target, but no peaks at higher energies. In contrast, the Doppler-shifted spectrum clearly shows a peak at 1297(18) keV corresponding to the first excited state in ^{44}S. To decide if this photopeak could be due to the decay of a 3^- state instead of a 2^+ state, we performed coupled channels calculations with the computer code ECIS88 [9] with standard collective model form factors and the optical model potential given for the ^{40}Ar+^{208}Pb reaction at 41 MeV/nucleon [10]. The calculated cross section for populating a 2^+ state was more than a factor of five larger than the 3^- cross section if one assumes identical excitation energies and coupling strengths for the two states. In the absence of a second photopeak in the spectrum we assume that the first excited state in ^{44}S corresponds to a 2^+ state.

The detector efficiencies were folded with the photon angular distributions [3] in the projectile and target frames to determine the photopeak efficiencies for photons emitted from the excited projectile and target nuclei. By comparing the photon yield of the first excited state in ^{44}S to the yield of the $7/2^+ \rightarrow g.s.$ transition in ^{197}Au we extracted a transition probability in ^{44}S relative to the known electromagnetic transition probability in ^{197}Au [11]. We verified in our data set for the known case of ^{42}S that this method gives identical results to a direct determination of the excitation cross section from the combination of the yield of γ-rays from the 2_1^+ state in ^{42}S, the number of ^{42}S nuclei observed in the phoswich detector, the gold target thickness, and the photon detection efficiency. For ^{44}S we obtained a reduced transition probability of $B(E2;0^+_{gs} \rightarrow 2^+_1) = 314(88)$ e^{2}fm^4. The prescription of Raman *et al.* [12] can be used to calculate the reduced quadrupole deformation parameter[1] β_2 from $B(E2;0^+_{gs} \rightarrow 2^+_1)$,

$$\beta_2 = 4\pi[B(E2;0^+_{gs} \rightarrow 2^+_1)]^{(1/2)}/(3ZR_0^2e), \tag{1}$$

where $R_0 = 1.2A^{1/3}$ fm and $B(E2;0^+_{gs} \rightarrow 2^+_1)$ is in units of e^{2}fm^4. For ^{44}S we obtain $|\beta_2^{\mathrm{exp}}| = 0.258(36)$.

Naively, the $N = 28$ isotones are expected to be spherical because this neutron number corresponds to a major shell closure. However, the collective $B(E2;0^+_{g.s.} \rightarrow 2^+_1)$ value in ^{44}S, as well as other collective results found in ^{46}Ar ($\beta_2 = 0.18(2)$) [3], ^{50}Ti ($\beta_2 = 0.17(1)$), ^{52}Cr ($\beta_2 = 0.22(1)$) and ^{54}Fe ($\beta_2 = 0.19(1)$) [13], indicate that the $N = 28$ shell closure is weaker than some of those found in heavier mass regions (for example, the uniformly non-collective nature of the 2^+_1 states of the $N < 82$ even-even Sn isotopes is well known). Thus, the structure of nuclei along $N = 28$ is determined by a subtle interplay between the proton configurations and the neutron shell closure, as suggested by Werner *et al.* [1]. These authors emphasized the role of $1f_{7/2} \rightarrow fp$ core breaking in determining the deformations of nuclei near ^{44}S.

In Ref. [1], the authors used two self-consistent mean field techniques to calculate the ground state quadrupole deformation[2] of ^{44}S, but the conclusions of the two calculations were significantly different from each other. The relativistic mean field (RMF) calculation

---

[1]We use the symbol β_2 to indicate reduced quadrupole deformation parameters calculated from transition probabilities in contrast to β_Q, which indicates reduced quadrupole deformation parameters calculated from the quadrupole moment Q_0 of the 2^+ state as discussed later in the text.

[2]It should be noted that Werner *et al.* published [1] quadrupole mass deformations while the present experiment is only sensitive to the electromagnetic interaction and thus to proton deformations. However, Werner *et al.* also show that $^{40-44}$S are close to isoscalar in their models and that isovector effects become important only for $N > 28$.

predicted a statically deformed prolate ground state with $\beta_2 = 0.31$, while the Skyrme Hartree-Fock (HF) calculation gave a gamma-soft shape with a small quadrupole deformation ($\beta_2 = 0.13$). While the present measurement cannot distinguish between static and dynamic deformations, the experimental result appears to favor the larger deformation calculated with the RMF method.

The dramatic shape changes among the $N = 20$ isotones around ^{32}Mg have been reproduced by several investigators using shell model calculations [15–18], and we have obtained similarly the $B(E2; 0^+_{g.s.} \rightarrow 2^+_1)$ value in a recent calculation for ^{44}S. The calculation for ^{44}S was carried out in a model space in which the protons occupy the $0d_{5/2}$, $0d_{3/2}$ and $1s_{1/2}$ (sd) orbitals and the neutrons occupy the $0f_{7/2}$ and $1p_{3/2}$ orbitals. If the $0f_{5/2}$ and $1p_{1/2}$ neutron orbitals had been included, the model space would have been too large for the available computing resources. Calculations using this truncation were tested for ^{46}Ar and ^{48}Ca by comparing the results to those using the full pf model space, and the resulting orbital occupations and excitation energies of the 2^+_1 states were very similar. We use the Wildenthal sd-shell interaction [19], the FPD6 pf-shell interaction [20] and the WBMB $sd-pf$ cross-shell interaction [16]. The cross-shell interaction successfully reproduces the properties of the $N = 20 - 22$ nuclei, including the large deformation in the ground state of ^{32}Mg [16]. The $B(E2)$ values are calculated using a proton effective charge of $e_p = 1.35e$ and a neutron effective charge of $e_n = 0.65e$, which were chosen to reproduce the strengths of the proton sd-shell E2 transitions in ^{36}S and ^{38}Ar [21] and the neutron pf-shell E2 transitions in ^{48}Ca [22]. These effective charges are consistent with the analysis of other E2 transitions in the sd [19] and pf shells [20]. In ref. [22] a larger neutron effective charge of $e_n = 0.9e$ was required because the fp shell truncation was more severe than the one used here (in [22] only one particle was allowed to be excited out of the $f_{7/2}$ shell). (The values of effective charge quoted in [3] are incorrect and should be replaced by those discussed above.)

Figure 3 compares the measured reduced quadrupole deformation parameters $|\beta_2|$ and 2^+_1 state energies in the sulfur isotopes with the self consistent mean-field results of Werner *et al.* [1] and the present shell model results. The experimental quadrupole deformations are well reproduced by the RMF calculations of Werner *et al.* for the neutron rich A=40, 42 and 44 sulfur isotopes. Our shell model calculations give good overall agreement for the $N = 20 - 26$ sulfur isotopes for both the energies and quadrupole deformations of the first excited 2_1^+ states.

The mean-field calculations of reference [1] consider only static deformations with a fixed intrinsic shape and with no angular momentum projection. For these static deformations there is only one intrinsic shape, and the $B(E2; 0^+_{g.s.} \to 2^+)$ value and the quadrupole moment of the 2^+ state are geometrically related; β_2 (from the B(E2) value) $= \beta_Q$ (from the quadrupole moment). The large-basis shell-model wave functions have good angular momentum and allow for the possibility of mixing between various deformations as well as for vibrational (dynamic) excitations. With the shell-model wave functions we calculated the quadrupole moment $Q(2^+)$ of the 2^+ states, and have used this to extract β_Q via the static relationship (see e.g. [1])

$$Q_0 = -(2/7)Q(2^+) = \sqrt{(5/\pi)}\, Z < r_p^2 > \beta_Q. \tag{2}$$

The results are given in table I. For ^{40}S and ^{42}S, $\beta_2 \approx \beta_Q$ and β_Q is positive, consistent with a prolate deformed configuration. However, for ^{44}S, β_Q is very small and thus close to the purely vibrational limit. As discussed in [1], the prolate and oblate SIII-HF mean-field configurations are nearly degenerate for ^{40,42,44}S and the calculations do not allow for configuration mixing and angular momentum projection. The RMF calculation of [1] strongly favors a prolate deformation for all of these nuclei. Thus, even though the β_2 values are similar for the large-basis shell model and RMF calculations for ^{44}S, the structure is rather different, and the present experiment which only measures $|\beta_2|$ cannot distinguish between them. Further experiments on the properties of neighboring odd-even nuclei should should allow one to distinguish between the static deformed structure of the RMF calculation and the vibrational structure of the shell-model calculation. An experimental identification of the location of the 4^+ state in ^{44}S would also elucidate this question.

All of the above theoretical calculations are sensitive to the assumed single-particle energies. The difference between the SIII-HF and RMF calculations is due to a difference in the single-particle energies near the fermi surface [1], and neither interaction has been adjusted to reproduce the single-particle energies specifically for this mass region. The large-basis shell-model calculations should be more realistic in this respect since they are derived from interactions [16,19,20] which are designed to reproduce the observed proton and neutron single-particle energies in the nearby semi-closed shell nuclei ^{40}Ca and ^{48}Ca.

In summary, the energy and $B(E2;0^+_{gs} \rightarrow 2^+_1)$ value of the 2^+_1 state of ^{44}S have been measured using intermediate-energy Coulomb excitation. The $B(E2;0^+_{g.s.} \rightarrow 2^+_1)$ value demonstrates that ^{44}S has a collective nature, although $|\beta_2|$ is smaller than in ^{40,42}S. The observed collectivity in ^{44}S can be reproduced with the RMF calculations of Werner *et al.* [1] which predict large static deformations for $^{40-44}$S and by shell model calculations using empirical interactions. The shell model calculations suggest that the collectivity in ^{44}S has a vibrational origin, while ^{40,42}S have large static deformations.

This work was supported by the National Science Foundation under Grant Nos. PHY-9528844, PHY-9523974 and PHY-9403666.

REFERENCES

[1] T.R. Werner et al., Phys. Lett. B 335 (1994) 259; Nucl. Phys. A 597 (1996) 327.

[2] A. Winther and K. Alder, Nucl. Phys. A 319 (1979) 518.

[3] H. Scheit et al., Phys. Rev. Lett. 77 (1996) 3967.

[4] R. Anne et al., Z. Phys. A 352 (1995) 397.

[5] T. Motobayashi et al., Phys. Lett. B 346 (1995) 9.

[6] R. Harkewicz, Rev. Sci. Instr. 67 (1996) 2176.

[7] B.M. Sherrill et al., Nucl. Instr. Meth. B 56 (1991) 1106.

[8] T. Glasmacher, P. Thirolf and H. Scheit (to be published).

[9] J. Raynal, Computer code ECIS88, unpublished.

[10] T. Suomijärvi *et al.*, Nucl. Phys. A **509**, 369 (1990).

[11] C. Zhou et al., Nucl. Data Sheets 76 (1995) 399.

[12] S. Raman et al., Phys. Rev. C 43 (1991) 556.

[13] S. Raman et al., At. Data Nucl. Data Tables 36 (1987) 1.

[14] V.A. Chepurnov, Yad. Fiz. 6 (1967) 955.

[15] A. Poves and J. Retamosa, Phys. Lett B 184 (1987) 311; A. Poves and J. Retamosa, Nucl. Phys. A 571 (1994) 221.

[16] E.K. Warburton, J.A. Becker, and B.A. Brown, Phys. Rev. C 41 (1990) 1147.

[17] K. Heyde and J.L. Wood, J. Phys. G 17 (1991) 135.

[18] N. Fukunishi, T. Otsuka, and T. Sebe, Phys. Lett. B 296 (1992) 279.

[19] B.A. Brown and B.H. Wildenthal, Ann. Rev. Nucl. Sci. 38 (1988) 29.

[20] W.A. Richter et al., Nucl. Phys. A 523 (1991) 325.

[21] P.M. Endt, Nucl. Phys. A 521 (1990) 1.

[22] G. Kraus et al., Phys. Rev. Lett. 73 (1994) 1773.

FIGURES

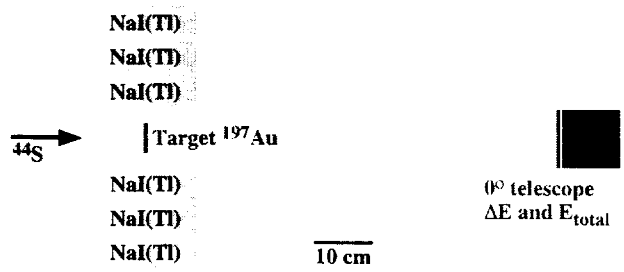

FIG. 1. Schematic setup of the secondary target area. The NaI(Tl) detectors and their relative positions to the target are indicated. The distance between the secondary target and the 0° telescope is 72 cm and limits the acceptance of scattered particles to scattering angles of $\theta_{\text{lab}} < 4.05°$. The lead shielding and two parallel plate avalanche counters used for beam tracking located 1 m and 2 m before the secondary target are not shown.

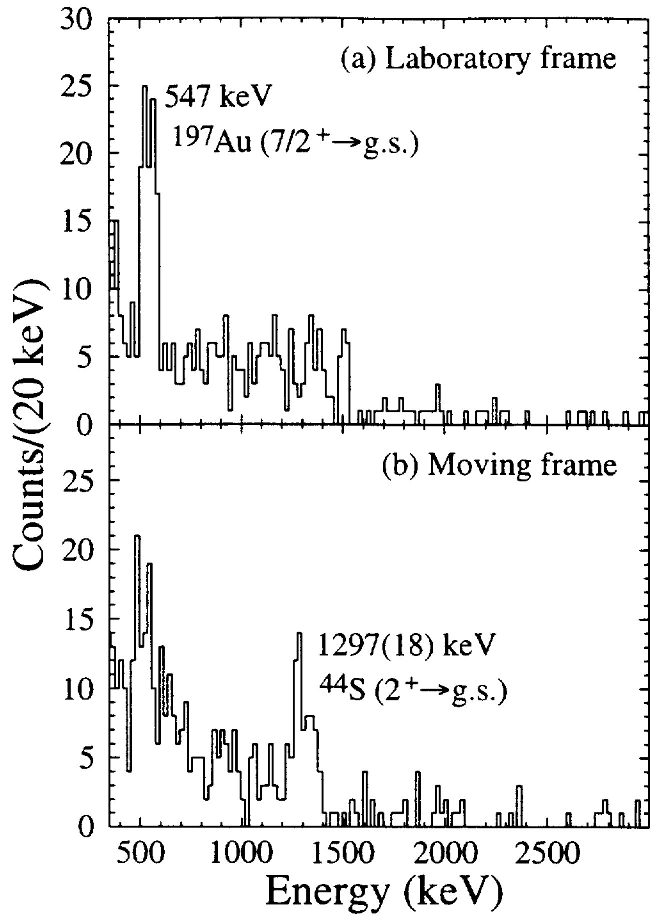

FIG. 2. The upper panel (a) contains the photon spectrum in the target frame. The 547 keV ($7/2^+ \rightarrow g.s.$) transition in the ^{197}Au target is visible as a peak, while the ($2^+ \rightarrow g.s.$) transitions in the projectile is very broad. The lower panel (b) contains the same energy spectrum, but Doppler-shifted into the projectile frame ($v = 0.276c$) on an event-by-event basis. The transition corresponding to the first excited state in ^{44}S becomes visible.

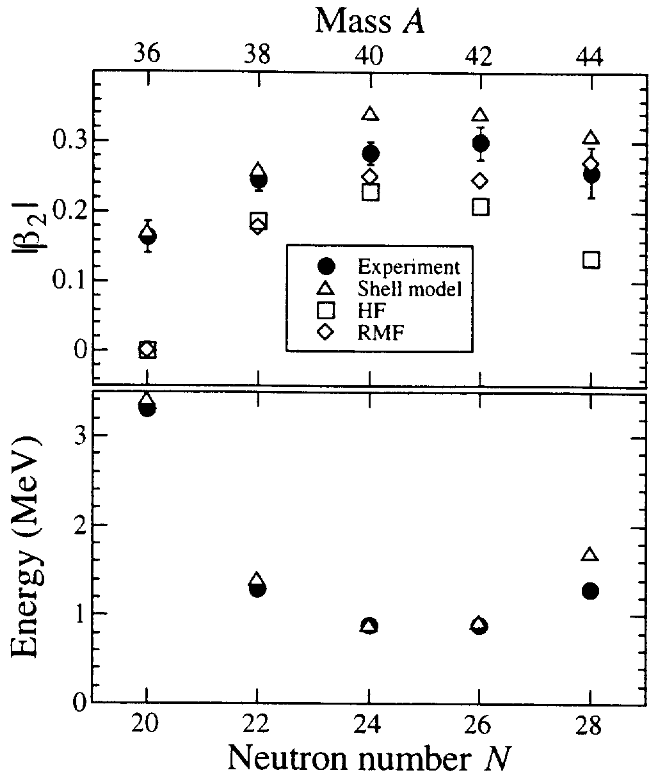

FIG. 3. A comparison of experimental values of the reduced quadrupole deformation parameters $|\beta_2|$ and the energies of the first excited states for the $N = 20 - 28$ sulfur isotopes $^{36}S-^{44}S$ to the nuclear models discussed in the text.

TABLES

TABLE I. Reduced static quadrupole deformation parameters (β_Q^p, β_Q^n, β_Q^A) calculated with the shell model from the quadrupole moment $Q_0(2^+)$ of the 2^+ state (first three columns) compared to deformation parameters calculated from the $0^+ \rightarrow 2^+$ transition probablities (β_2^p, β_2^n, β_2^A) and measured values (from refs. [13] (^{36}S), [3] ($^{38-42}$S), and this experiment (^{44}S)). The relation between B(E2↑) and β_2 is given in equation 1.

	β_Q^p	β_Q^n	β_Q^A	$\|\beta_2^p\|$	$\|\beta_2^n\|$	$\|\beta_2^A\|$	B(E2↑)^{exp} (e^{2}fm^4)	$\|\beta_2^{exp}\|$
^{36}S	0.16	0.07	0.12	0.17	0.07	0.12	96(26)	0.16(2)
^{38}S	0.15	0.15	0.15	0.26	0.24	0.25	235(30)	0.25(2)
^{40}S	0.31	0.29	0.30	0.34	0.29	0.31	334(36)	0.28(2)
^{42}S	0.32	0.26	0.29	0.34	0.25	0.29	397(41)	0.30(2)
^{44}S	0.08	0.01	0.03	0.31	0.19	0.24	314(88)	0.26(4)